IOP Conf. Series: Materials Science and Engineering **416** (2018) 012042 doi:10.1088/1757-899X/416/1/012042

Assessment of Mass Variation by Vibration-based Methods

L Barboni[1], GR Gillich[1,*] and ZI Korka[1]

[1]"Eftimie Murgu" University of Resita

[*]Corresponding author: gr.gillich@uem.ro

Abstract. We present in this paper a study regarding the effect of mass variation on the vibration response of a beam-like structure. During operation, the structures can be exposed to the action of supplementary masses which additionally load them and change their dynamic behavior. These loads can be therefore observed and assessed from the changes in the natural frequencies since the mass increase leads to a frequency decrease. To find the effect of increasing the mass of a beam slice, we used the law of conservation of mechanical energy. The total stored energy is unaltered from the mass change and equals the total kinetic energy. Hence, increasing a slice's mass has as a consequence the velocity decreases, thus the frequency decreases. We succeed to demonstrate that the slice position in the beam is crucial for the frequency change in each bending mode and found a relation for the calculus of a coefficient that can be used to predict the frequency changes due to a local mass alteration. The relation was successfully tested against experiments.

1. Introduction

During operation, structural elements are subject to designed or accidental loads which can act temporary or permanently. Undesired quasi-permanent loads are, for example, those produced by adherent particles or, especially for wood or similar elements, by moisture. These loads, since not considered in the design process, can affect the safety of the entire structure. Because it is hard to evaluate such accidental loads by direct measurements, engineers face the important task of developing indirect methods to assess supplementary masses on structural elements.

The literature is rich in papers presenting vibration-based methods used nowadays to assess changes in structures [1]-[5]. Most of such methods, dedicated to identifying the structure region where mass and stiffness are affected, are based on measuring the changes in the natural frequencies [6]. A technique involving sensor clusters which simultaneously detect stiffness and mass changes is presented in [7]. How the occurrence of mass changes in satellites can be performed, is shown in [8], while the effect of a moving mass represented by a vehicle on the measured modal parameters of a bridge from traffic-induced excitation is described in [9]. The last two mentioned papers consider just mass changes because the structural stiffness is not affected by the additional mass. In [10], a different approach is presented, the link between the mass and the structure being done by a spring system.

Our previous research was dedicated to contrive relations that precisely predict the frequency changes due to mass or stiffness alteration in a slim beam element [11]-[14]. It was found that the global stiffness decrease [15] or the total energy stored in the beam [16] has to be considered if prediction of natural frequency changes is approached. The research presented in this paper takes into account exclusively the influence of local mass increase on the natural frequencies and make use of the principle of conservation of the mechanical energy. The finding is used to define patterns usable in the process of assessing mass variation.

Content from this work may be used under the terms of the Creative Commons Attribution 3.0 licence. Any further distribution of this work must maintain attribution to the author(s) and the title of the work, journal citation and DOI.
Published under licence by IOP Publishing Ltd

2. Materials and methods

As the changes of the natural frequencies are used to evaluate the condition of beam-like structures, the paper aims to present a relationships elaborated by the authors, which is able to assess any mass change. For exemplification, a cantilever beam which is supporting an additional mass m_a placed at a certain distance is presented. The analysed beam (Figure 1.a) is made of steel and has a prismatic shape defined by length L = 1000 mm, height H = 5 mm and width B = 50 mm. As such, the main elements defining the stiffness of the steel bar are: the area of the cross section $A = B \cdot H$ and the moment of inertia of plain area $I = (B \cdot H^3)/12$. The other factors which are characterizing the mechanical properties of the beam are: the longitudinal elasticity modulus E, the Poisson's ratio ν and the volumetric mass density ρ. Those values, taken from the software library, are indicated in Table 1.

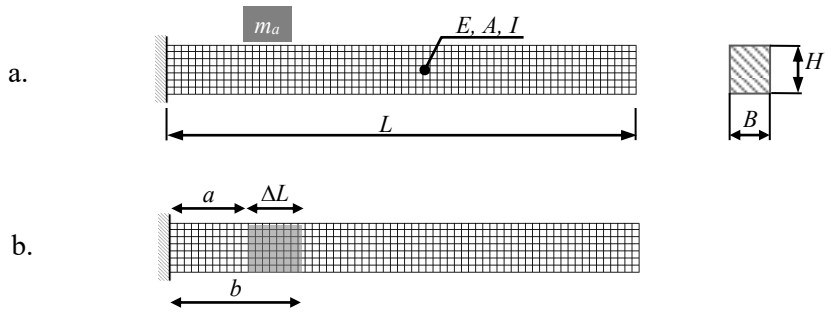


Figure 1. Cantilever beam with additional mass (a) and its FE model (b).

The analytic approach is based on conservation of the mechanical energy applied to the Euler-Bernoulli beam. How the frequency dependency on the non-uniform distributed beam mass was derived is presented in next section.

Table 1. Beam dimensions and material's physical-mechanical properties.

Mass density original beam ρ [kg/mm^3]	Equiv. mass density (one additional mass) ρ_1 [kg/mm^3]	Equiv. mass density (two additional masses) ρ_2 [kg/mm^3]	Young modulus E [N/m^2]	Poisson ratio υ [-]
7850	12637.5	17425	$2 \cdot 10^{11}$	0.3

The research presented in this paper took place in three stages. In the first stage, we calculated the natural frequencies of the beam and, based on the relationship we propose in the next section, the modified natural frequencies of the beam after placing one additional mass m_a = 47.875 g and two additional masses $2 \cdot m_a$= 95.75 g respectively.

In the second stage, to test the contrived relation, the natural frequencies were found using the modal analysis module of ANSYS. A finite element (FE) model meshed by using hexahedral elements with maximum edge size 2 mm was created, resulting in about 37500 elements. Instead of the additional masses, the density of the corresponding beam segment, located between a = 300 mm and b = 340 mm, was increased (see Figure 1.b and equivalent mass densities in Table 1). The simulation was performed for the same two cases of additional masses as above described. To test the proposed relation, the coefficients considering mass position and weight were applied to the frequencies of the original beam and the estimated frequencies were compared with those attained by FEM.

In the last stage, in order to calibrate the FEM model, the natural frequencies were measured on the test stand shown in Figure 2. The clamping of the beam (1) was done with a universal vice (2), similar to those used on machine- tools. The additional masses were simulated by placing two annular magnets 3 on each bar side at the required distance from the fixed end. The use of a magnetic weight has the advantage of not hampering the deformation of the bar in the contact area.

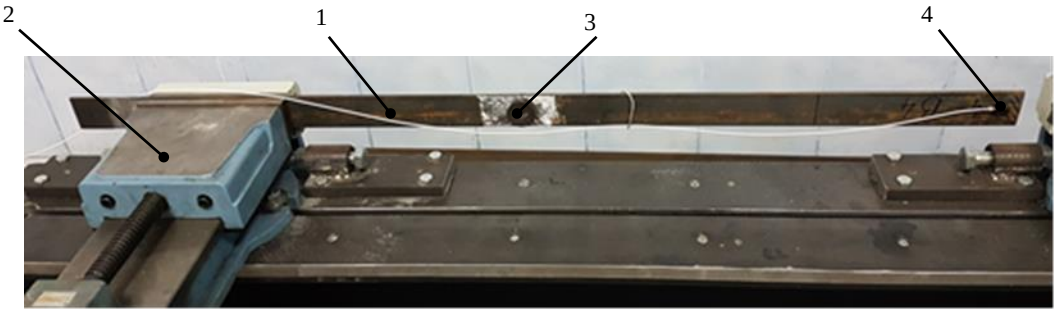


Figure 2. Beam with additional mass prepared for experimental tests.

For collecting the vibration signals, a Kistler 8772A10 accelerometer (4) was employed, which was connected through a signal acquisition module NI 9234 to a computer running a special application designed in LabView software [17]. The application was developed in order to ensure and exact processing of the collected data and for a precise labelling of the vibration frequencies [18].

3. Deriving the natural frequencies of the beam loaded with an additional mass

For a cantilever beam, the natural frequencies f_i for the bending vibration modes are calculated with the relationship:

$$f_i = \frac{\alpha_i^2}{2\pi}\left(\frac{EI}{mL^3}\right)^{1/2}, \tag{1}$$

where: m is the mass of the beam and α_i are the wave numbers for the beam, which are calculated from the characteristic vibration equation:

$$\cos\alpha\cosh\alpha + 1 = 0\,. \tag{2}$$

Now, let's consider an additional mass m_a placed on the beam at a distance x from the fixed end (Figure 1a). Reducing the additional mass m_a to the width B and the height H of the beam, on a segment of length ΔL, the volumetric mass density of the beam is considered to be increased, while maintaining the stiffness constant (Figure 1b). On the rest of the beam, the mass density remains unchanged. The model shown in Figure 1b is adopted to derive the consequence on the natural frequencies of the additional mass placed on the beam.

First, the own mass of the cantilever beam is neglected. Considering a mass m_P placed at a distance x from the fixed end of the beam, it covers a distance $w_i(x)$ in a quarter-period $T_i/4$. Another mass m_E placed at the free end of the beam covers in the same period of time the distance $w_i(L)$. These distances are connected on the bending vibration mode shape of the cantilever beam, being calculated as:

$$w_i(x) = \cosh\alpha_i x - \cos\alpha_i x - \frac{\cos\alpha_i L + \cosh\alpha_i L}{\sin\alpha_i L + \sinh\alpha_i L}(\sin\alpha_i x - \sinh\alpha_i x)\,. \tag{3}$$

Figure 3 shows the distances $w_i(x)$ and $w_i(L)$ computed for the vibration modes 1 and 3. The kinetic energy of the mass m_P may be calculated as:

$$U_{Ki}(x) = \frac{m_p}{2}\left[\frac{w_i(x)}{T_i}\right]^2, \tag{4}$$

with T_i the period of the oscillation. The mass m_E, the kinetic energy can be expressed as:

$$U_{Ki}(L) = \frac{m_E}{2}\left[\frac{w_i(L)}{T_i}\right]^2, \tag{5}$$

In order to obtain in both cases the same natural frequencies, the kinetic energies expressed by Eq. 4 and 5 have to be equal. Thus, the dependence between the two masses, for the i^{th} vibration mode, can be expressed as:

$$m_{Ei} = m_{Pi}\left[\frac{w_i(x)}{w_i(L)}\right]^2 = m_{Pi}[\bar{w}_i(x)]^2, \tag{6}$$

where $\bar{w}_i(x)$ stands for the dimensionless transverse displacement of a point situated at the length x from the fixed end. This proportion takes values between zero and one.

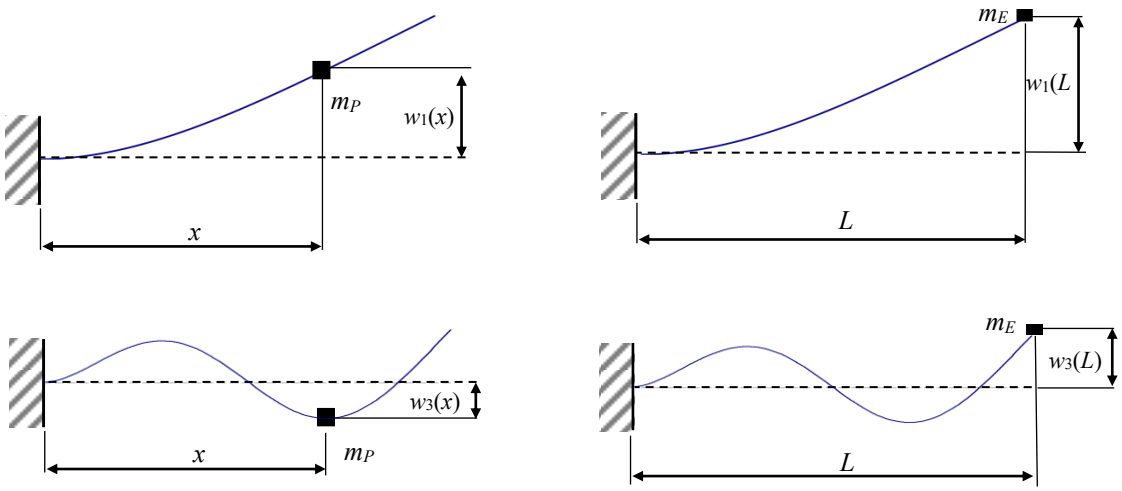


Figure 3. Displacements computed for vibration modes 1 and 3 at two dynamic systems with masses located in different positions.

Analysing Eq. 6, it can be concluded that for any mass located on a cantilever beam at a distance x from the fixed end, an equivalent mass situated on the free end may be assumed. The relation between these two masses is given by the square of the dimensionless transverse displacement $[\bar{w}_i(x)]^2$. That's why, for dynamic reasons, the equivalent mass of a beam may be obtained by adding the equivalent masses of all beam slices. Figure 4 illustrates this approach for bending vibration mode 3 of the beam.

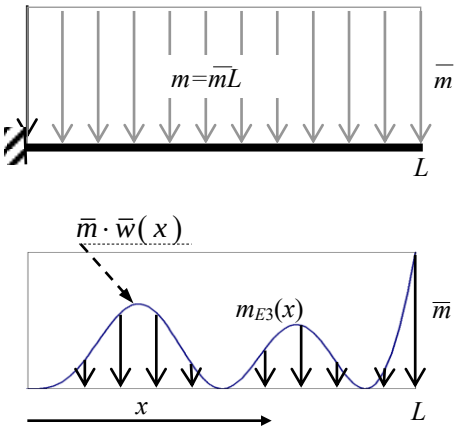


Figure 4. Cantilever beam statically load by a distributed inertial and the mass participation to the kinetic energy for vibration mode three.

Genuinely, the total equivalent specific mass m_i^{eq}, which corresponds to the i^{th} bending vibration mode is acquired by multiplying the specific mass of the beam $\bar{m}$ with the area located below the graph of the function $[\bar{w}_i(x)]^2$. Therefore, we have:

$$m_i^{eq} = \bar{m}L\int_0^L [\bar{w}_i(x)]^2 dx = 0.25\bar{m}L. \tag{7}$$

As the curves are having the same nature, the area located below the graph of the function $[\bar{w}_i(x)]^2$ is always 0.25 for each bending vibration mode. Consequently, the natural frequencies of the beam may be formulated by using the equivalent mass as:

$$f_i = \frac{\alpha_i^2}{2\pi}\left(\frac{EI}{\bar{m}L^4}\right)^{1/2} = \frac{\alpha_i^2}{2\pi}\left(\frac{EI}{4m_i^{eq}L^3}\right)^{1/2}. \tag{8}$$

Based on Eq. (7), the participation of any mass located along the beam to the total kinetic energy can be derived. The distance traveled over a quarter of the period T_i represents the contribution of each slice. For example, Figure 5 illustrates the mass participation to the total kinetic energy of 100 slices located along the beam for vibration mode three.

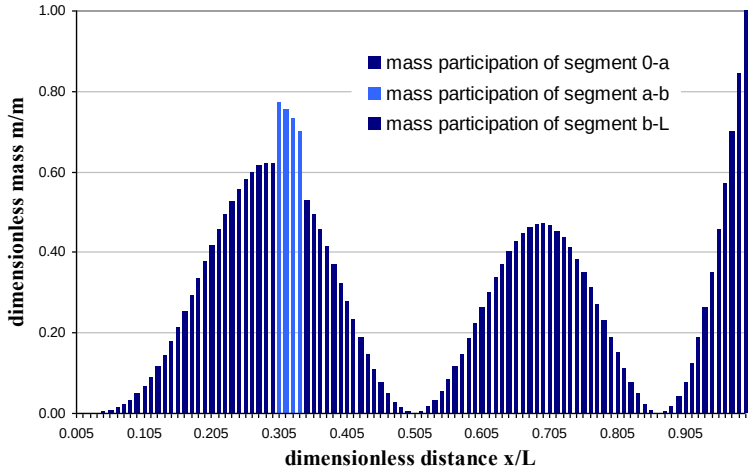


Figure 5. Mass participation to the total kinetic energy of 100 slices located along the beam for vibration mode three.

Next, let's consider that the specific mass of the beam increases on a length $\Delta L = b - a$, due to placing on the beam an additional mass m_a (see Figure 1). As a consequence, on that segment, the specific mass increases to $\bar{m}_a$. Thus, the equivalent mass contribution of this segment may be expressed as:

$$m_{ai}^{eq} = \bar{m}_a L\int_a^b [\bar{w}_i(x)]^2 dx = k_i^{a-b}\bar{m}_a L. \tag{9}$$

Similarly, the equivalent specific masses of the two segments located between *0* and *a*, respective *b* and *L*, are:

$$m_{i-1}^{eq} = \bar{m}L\int_0^a [\bar{w}_i(x)]^2 dx = k_i^{0-a}\bar{m}L, \tag{10a}$$

$$m_{i-3}^{eq} = \bar{m}L\int_b^L [\bar{w}_i(x)]^2 dx = k_i^{b-L}\bar{m}L. \tag{10b}$$

In case that the additional mass would be distributed along the whole bar length results $k_i^{0-L} = 0.25$. Presuming the beam maintains its stiffness constant, the increase of the mass density of the beam on the portion located between *a* and *b*, changes the natural frequencies of the bar as follows:

$$f_{Mi} = \frac{\alpha_i^2}{2\pi}\left(\frac{EI}{4(m_{i-1}^{eq} + m_{ai}^{eq} + m_{i-3}^{eq})L^3}\right)^{1/2}, \tag{11}$$

which may be also expressed as:

$$f_{Mi} = \frac{\alpha_i^2}{2\pi}\left(\frac{EI}{4(k_i^{0-a}\bar{m} + k_i^{a-b}\bar{m}_a + k_i^{b-L}\bar{m})L^4}\right)^{1/2}, \tag{12}$$

With regard to Eq. (8), one can write Eq. (12) as:

$$f_{Mi} = f_i\left(\frac{\bar{m}}{4(k_i^{0-a}\bar{m} + k_i^{a-b}\bar{m}_a + k_i^{b-L}\bar{m})}\right)^{1/2} = c_{Mi} f_i . \tag{13}$$

were c_{Mi} takes into account the existence of an additional mass m_a, and can be used to estimate the frequency for FEM and measurements. Forwards, the frequency decrease can be written as:

$$\Delta f_{Mi} = f_i\left[1 - \left(\frac{\bar{m}}{4(k_i^{0-a}\bar{m} + k_i^{a-b}\bar{m}_a + k_i^{b-L}\bar{m})}\right)^{1/2}\right] = (1 - c_{Mi}) f_i . \tag{14}$$

Consequentially, the relative frequency shift (RFS), which is obtained by dividing the frequency decrease to the initial frequency of the beam, in the corresponding vibration mode, becomes:

$$\Delta f_{Mi} = \frac{\Delta f_{Mi}}{f_i} = 1 - \left(\frac{\bar{m}}{4(k_i^{0-a}\bar{m} + k_i^{a-b}\bar{m}_a + k_i^{b-L}\bar{m})}\right)^{1/2} = 1 - c_{Mi} . \tag{15}$$

RFS can be found for several bending vibration modes; these define patterns able to characterize the occurrence of an additional mass of given dimension and position.

4. Results and discussion

The natural frequencies of the first six vibration modes for the original beam and for the beam on which was placed one (m_a) and two additional masses ($2 \cdot m_a$), respectively, are shown in Table 2. The natural frequencies were obtained by EM and experimental measurements.

Table 2. Natural frequencies obtained by FEM and experimental measurements.

Mode No.	FEM simulations results					Measurement results				
	Frequency [Hz]			RFS^{FEM} for beam with m_a [%]	RFS^{FEM} for beam with $2 \cdot m_a$ [%]	Frequency [Hz]			RFS^{meas} for beam with m_a [%]	RFS^{meas} for beam with $2 \cdot m_a$ [%]
	Original beam	Beam with m_a	Beam with $2 \cdot m_a$			Original beam	Beam with m_a	Beam with $2 \cdot m_a$		
1	4.0901	4.0852	4.0805	0.117	0.232	4.0806	4.0757	4.0711	0.105	0.221
2	25.627	25.236	24.859	1.525	2.996	24.701	24.326	24.027	1.514	2.725
3	71.757	69.963	68.397	2.500	4.682	70.61	68.897	67.498	2.426	4.406
4	140.63	140.02	139.5	0.433	0.803	138.22	137.67	137.14	0.398	0.781
5	232.53	230.88	229.43	0.709	1.333	232.39	230.87	229.53	0.654	1.231
6	347.46	340.28	334.64	2.066	3.689	341.52	335.17	330.04	1.859	3.361

Table 3. Frequencies estimated for the beam subjected to additional masses and the subsequent RFSs.

Mode No.	Orig. beam	Estimation - beam with m_a			Estimation - beam with $2 \cdot m_a$			Estimated RFS^{FEM}	
	Freq. [Hz]	c_{Mi} [-]	Freq. [Hz]	Error [%]	c_{Mi} [-]	Freq. [Hz]	Error [%]	Beam with m_a [%]	Beam with $2 \cdot m_a$ [%]
1	4.09	0.9988	4.0852	-0.0017	0.9976	4.0805	-0.0013	0.115	0.230
2	25.627	0.9847	25.236	-0.0024	0.9702	24.859	-0.0182	1.523	2.979
3	71.757	0.9743	69.963	0.0620	0.9506	68.397	0.2639	2.560	4.934
4	140.63	0.9955	140.02	0.0155	0.9910	139.50	0.0897	0.449	0.892
5	232.53	0.9923	230.88	0.0549	0.9848	229.43	0.1802	0.764	1.511
6	347.46	0.9774	340.28	0.1945	0.9563	334.64	0.7040	2.256	4.367

The values presented in Table 2 show that the RFS values obtained by FEM and experiments are very similar, which confirms the validity of the Eq. (15).

Table 3 exemplifies how the natural frequencies of a beam subjected to one or two additional masses can be estimated, starting from the values of the natural frequencies obtained by FEM on the original bar and applying the coefficient c_{Mi} and Eq. (13). One can see that the percentage differences between the estimated frequencies and those obtained by FEM are less than 1%. The table is completed with the RFS values obtained by estimation (calculus).

In order to highlight the differences between RFS values obtained by FEM and the estimated ones, Figure 6 provides two charts, each plotted for one, respectively two additional masses.

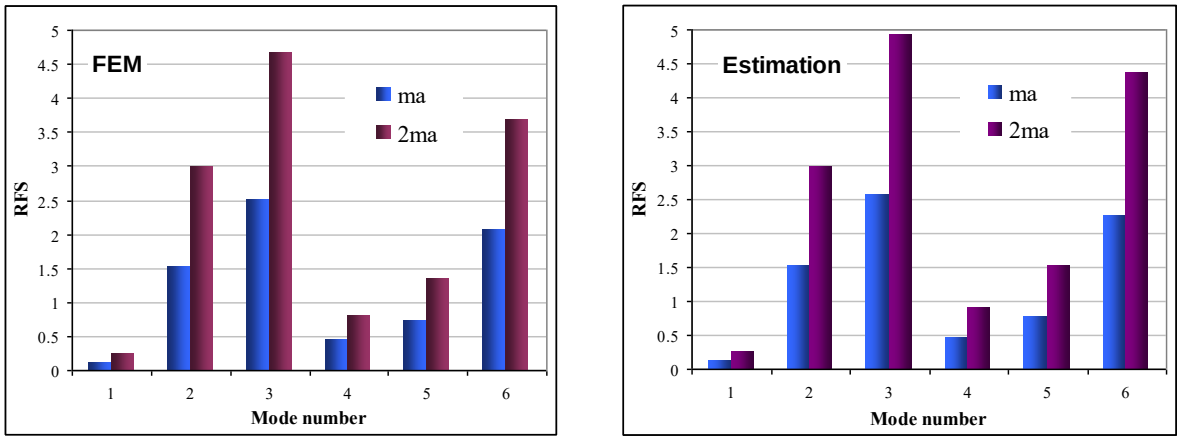


Figure 6. Relative frequency shifts for the case that one respectively two additional masses are placed on the beam segment between a = 300 mm and b = 340 mm; left graph represents the values obtained from FEM simulations while the right graph stay for the values obtained by applying Eq. (13).

A good equal was found by comparing the data directly resulted from FEM with the estimations. This further confirms the validity of the analytical formulas for the calculation of the frequencies.

5. Conclusion

A mathematical relation that allows the estimation of the natural frequencies of a beam which supports an additional mass was proposed herein. The relation contains a coefficient that can be calculated in respect to the position and size of the additional mass. It has practical utility in analytically determining of patterns if the natural frequencies of the continuous bar are known. The use of these patterns turns the position and size identification of the additional mass into an inverse problem.

The RFS values reflect changes in natural frequencies caused by the existence of an additional mass on the beam. The distribution of these values in vibration modes reflects the position of the additional mass on the beam. By normalization, it results a string of values ranging from 0 to 1, identical for any mass increase, just like in the case of beams subjected to stiffness loss [14].

6. References

[1] Zhou Y L, Qian X, Cao H and Wahab M A 2017 Damage detection in structures using frequency response functions ensemble with extended cosine based indicator *J. Phys. Conf. Ser.* **843** 012021
[2] Teodorescu-Draghicescu H, Stanciu A, Vlase S, Scutaru L, Calin M R and Serbina L 2011 Finite element method analysis of some fibre-reinforced composite laminates *Optoelectron. Adv. Mat.* **5**(7) 782-785
[3] Gillich G R, Birdeanu E D, Gillich N, Amariei D, Iancu V and Jurcau C S 2009 Detection of damages in simple elements *Annals of DAAM & Proc. of 20th Intern. Symp.* **20**(1) 623-625
[4] Bighamian R and Mirdamadi H R 2013 Input/output system identification of simultaneous mass/stiffness damage assessment using discrete-time pulse responses, differential evolution algorithm, and equivalent virtual damped SDOF *Struct. Control Hlth.* **20**(4) 576-592
[5] Vlase S 2012 Dynamical response of a multibody system with flexible elements with a general three-dimensional motion *Rom J. Phys.* **57**(3-4) 676-693
[6] Doebling S W, Farrar C R, Prime M B and Shevitz D W 1996 *Damage Identification and Health Monitoring of Structural Systems from Changes in Their Vibration Characteristics: A Literature Review* (Report LA-12767-MS, Los Alamos National Laboratory, NM: USA)
[7] Mei Q and Gül M 2014 Novel Sensor Clustering–Based Approach for Simultaneous Detection of Stiffness and Mass Changes Using Output-Only Data *J. Struct. Eng.* **141** (10) 04014237
[8] Kim C Y, Kim N S, Yoon J G and Jung D S 1999 Effect of vehicle mass on the measured dynamic characteristics of bridges from traffic-induced vibration test. *SPIE Proceedings* 1106-1111
[9] Maji A and Vernon B 2012 Vibration-based monitoring to detect mass changes in satellites, *Proc. SPIE* **8348** Health Monitoring of Structural and Biological Systems 83481G
[10] Wu J J 2006 Use of equivalent mass method for free vibration analyses of a beam carrying multiple two-dof spring-mass systems with inertia effect of the helical springs considered *Int. J. Numer. Meth. Eng.* **65**(5) 653-678
[11] Negru I, Praisach Z I, Gillich G R and Vasile O 2015 About the neutral axis distortion due to cracks and its influence upon the beams natural frequencies *Rom. J. Acoust. Vib.* **12**(1) 35-38
[12] Gillich G R, Wahab M A, Praisach Z I and Ntakpe J L 2014 The influence of transversal crack geometry on the frequency changes of beams *Proc. of Int. Conf. on Noise and Vibration Engineering ISMA2014* (Leuven, Belgium) 485-498
[13] Gillich G R, Praisach Z I, Wahab M A, Gillich N, Mituletu I C and Nitescu C 2016 Free Vibration of a Perfectly Clamped-Free Beam with Stepwise Eccentric Distributed Masses *Shock Vib*. **2016** 2086274
[14] Gillich G R, Praisach Z I and Negru I 2012 Damages Influence on Dynamic Behaviour of Composite Structures Reinforced with Continuous Fibers *Mater. Plast.* **49**(3) 186-191
[15] Nitescu C, Gillich G R, Wahab M A, Manescu T and Korka Z I 2017 Damage severity estimation from the global stiffness decrease *J. Phys. Conf. Ser.* **842** 012034
[16] Gillich G R, Tufoi M, Korka Z I, Stanciu E and Petrica A 2016 The Relations between Deflection, Stored Energy and Natural Frequencies, with Application in Damage Detection *Rom. J. Acoust. Vib.* **13**(2) 87-93
[17] Gillich G R, Frunzaverde D, Gillich N and Amariei D 2010 The use of virtual instruments in engineering education *Procedia Soc. Behav. Sci.* 2(2) 3806-3810
[18] Gillich G R, Mitletu I C, Praisach Z I, Negru I and Tufoi M 2016 A method to enhance frequency readability for early damage detection *J. Vibr. Eng. Technol.* **3**(5) 637- 652